Biochemical and Biophysical Research Communications 391 (2010) 841–845

Contents lists available at ScienceDirect

Biochemical and Biophysical Research Communications

journal homepage: www.elsevier.com/locate/ybbrc

Clustering of protein kinase A-dependent CFTR chloride channels in the sarcolemma of guinea-pig ventricular myocytes

Andrew F. James [a,b,*], Razshan Z. Sabirov [a,c], Yasunobu Okada [a]

[a] Department of Cell Physiology, National Institute for Physiological Sciences, Okazaki 444-8585, Japan
[b] Cardiovascular Research Laboratories, Bristol Heart Institute, Department of Physiology & Pharmacology, University of Bristol, Bristol BS8 1TD, UK
[c] Laboratory of Molecular Physiology, Institute of Physiology & Biophysics, Acad. Sci. RUz and Department of Biophysics, National University, Niyazova 1, 100095 Tashkent, Uzbekistan

ARTICLE INFO

Article history:
Received 17 November 2009
Available online 27 November 2009

Keywords:
Cardiac myocytes
CFTR
PKA-dependent Cl^- channel
Smart patch clamp

ABSTRACT

Cardiac myocytes express protein kinase A-dependent Cl^- (Cl_{PKA}) channels that are thought to represent cardiac expression of CFTR. In the present study, the 'Smart' patch clamp technique was used to investigate the distribution of Cl_{PKA} channels at the cell surface of isolated guinea-pig ventricular myocytes. Imaging the cell surface using scanning ion conductance microscopy allowed the identification of the mouths to t-tubules and lateral z-grooves with a spacing of 1.86 μm. Cell-attached patch clamp recordings were made from specified locations within the imaged area. Perfusion of the cells with an activating cocktail of isoprenaline (5 μM), forskolin (10 μM) and isobutylmethylxanthine (50 μM) activated large, noisy anion-selective currents in which unitary channel currents could not be identified. Currents were recorded both from within z-grooves and in the inter-groove region but not at the mouths of t-tubules. Power spectral and noise analyses indicated the involvement of 13.5 pS channels occurring in clusters of >50 channels. Channel activity was lost on excision of the patch from the cell but could be recovered in inside-out excised patches by application of the catalytic subunit of PKA. These results suggest that CFTR Cl_{PKA} channels occur in clusters in the sarcolemma of guinea-pig ventricular myocytes; there was no evidence of a heterogeneous distribution of clusters between the z-grooves and the inter-groove region.

Introduction

Cardiac myocytes possess a chloride conductance activated by G-protein coupled receptors via cyclic AMP signaling pathways [1–4]. The protein kinase A (PKA)-dependent Cl^- channels (Cl_{PKA}) underlying this conductance are thought to represent the cardiac expression of the cystic fibrosis transmembrane conductance regulator protein, CFTR [5–8]. Cardiac Cl_{PKA} channel currents can be activated via G_s-coupled receptors, such as β-adrenoceptors and histamine H_2-receptors, and the activated currents inhibited via G_i-coupled receptors, such as muscarinic receptors, α_1-adrenoceptors and endothelin ET_A receptors [1,9–11]. The equilibrium potential for Cl^- ions in cardiac muscle is thought to be in the range −65 to −40 mV, so that activation of a Cl^- conductance can be expected to contribute depolarizing inward current at the resting membrane potential and repolarizing outward current during the plateau phase of the action potential, with the predominant effect of Cl_{PKA} channel activation being to shorten the action potential duration (APD) [1,5,12]. It has therefore been suggested that cardiac Cl_{PKA} CFTR channels may function to control the action potential in the face of the APD prolonging effect of β-adrenoceptor-mediated potentiation of the L-type Ca^{2+} channel current [1].

There is accumulating evidence that many ion channels and transporters are heterogeneously distributed within the cardiac sarcolemma, their localization being specific to their function and regulation. The sarcolemma itself is quite inhomogeneous, possessing t-tubules, which are relatively large diameter (*i.e.* 100–450 nm) invaginations of the cell membrane that lead to a branching network that plays a key role in excitation–contraction (EC) coupling [13,14], and caveolae, that are more shallow invaginations of the sarcolemma (*i.e.* 50–100 nm diameter) enriched in cholesterol in which various membrane and signaling proteins may be co-localized [15,16]. The t-tubule membrane is particularly enriched in ion channels and transporters key to EC coupling, including L-type Ca^{2+} channels and the Na^+/Ca^{2+} exchanger [17–19]. Caveolae play an important role in the compartmentalization of cyclic AMP signaling [16,20–22]. There is also evidence that interaction with scaffolding proteins, such as A-kinase anchoring protein (AKAP) and ezrin binding proteins, play an important role in the localization and anchoring of cardiac ion channels in macromolecular signaling complexes [23–25]. CFTR channels possess a PDZ-binding domain in the C-terminus that allows the channels to form immobilized macromolecular complexes and plays a role

* Corresponding author. Address: Department of Cell Physiology, National Institute for Physiological Sciences, Okazaki 444-8585, Japan. Fax: +44 117 331 2288.
E-mail address: a.james@bristol.ac.uk (A.F. James).

0006-291X/$ - see front matter © 2009 Elsevier Inc. All rights reserved.
doi:10.1016/j.bbrc.2009.11.149

in the membrane localization of the channels [26–28]. However, while there is considerable data regarding the localization of other cardiac ion channels, there is very little information regarding the distribution of Cl_{PKA} channels in the cardiac sarcolemma. The objective of this study was to use the 'Smart' patch clamp technique, which has been used to demonstrate the localization of cardiac L-type Ca^{2+} channels and ATP-sensitive K^+ channels to the mouths of t-tubules [19,29], to examine the distribution of Cl_{PKA} at the cardiac myocyte cell surface.

Methods

Isolation of guinea-pig ventricular myocytes. Cardiac myocytes were isolated from the left ventricle of adult male guinea-pigs (~400 g, Japan SLC, Hamamatsu, Japan) by retrograde perfusion of the heart with a collagenase-containing Tyrode's solution via the aorta as described previously [6]. Cells were stored until use in a 'KB' solution at 4 °C [30]. Experiments were performed within 12 h of cell isolation. All procedures were performed according to the Guidelines for the Care and Use of Laboratory Animals of the Physiological Society of Japan. Experimental protocols were reviewed and approved by the Ethics Review Committee for Animal Care and Experimentation of the National Institutes of Natural Sciences.

'Smart' patch clamp: combined scanning ion conductance imaging and patch clamp recording. Cells were superfused with Tyrode's solution containing (in mM): NaCl 145, KCl 5.4, $MgCl_2$ 1.2, $CaCl_2$ 1, D-glucose 11, 4-(2-hydroxyethyl)-1-piperazineethanesulfonic acid (Hepes) 10 at pH 7.4. Experiments were performed at room temperature (~25 °C) using the 'Smart' patch clamp approach [29]. Patch pipettes were pulled from borosilicate glass (Summit Medical, Tokyo, Japan) and had tip resistances of 23.5 ± 1.3 MΩ (n = 36) when filled with the pipette solution containing (in mM): *N*-methyl-D-glutamine chloride (NMDG-Cl) 146, $MgCl_2$ 2, Hepes 5, pH 7.5. Using the patch pipette as a conductance probe, 10 μm × 10 μm square images of the myocyte surface were recorded to the hard drive of a PC using SICM software (Ionscope Ltd., London, UK) as reported previously [29,31]. Images were analyzed using Imag software (Ionscope Ltd., London, UK). The profile at the cell surface was assessed from the relative height/depth at lines drawn along the longitudinal axis of the cell. After formation of the image, the pipette was directed to a location on the cell surface specified by co-ordinates within the image and an attempt was made to form a giga-seal. Recordings were then made in the cell-attached configuration of the patch clamp technique. Cells were superfused with a cocktail of agonists in Tyrode's solution, including the β-adrenoceptor agonist, isoprenaline (ISO, 5 μM), the adenylyl cyclase activator, forskolin (FSK, 10 μM) and the phosphodiesterase inhibitor, isobutylmethylxanthine (IBMX, 50 μM). In some cells, following recordings of currents in the cell-attached configuration, the patch was excised from the membrane and currents recorded in the inside-out configuration. The cytosolic surface of excised patches was superfused with an excised patch recording solution containing (in mM): NMDG-Cl 146, $MgCl_2$ 2, Hepes 5, pH 7.5. The catalytic subunit of protein kinase A (PKA; Sigma, Japan) was applied to the cytosolic surface of patches at 20 U/ml in a modified excised patch recording solution in which $MgCl_2$ had been substituted with equimolar Mg-ATP. Current recordings were made using an Axopatch 200B (Molecular Devices, CA, USA), low pass filtered through an 8-pole Bessel filter with a corner frequency (f_c) of 1 kHz and recorded to the hard drive of a PC using pClamp 9 software (Molecular Devices, CA, USA) at a sampling frequency of 2 or 5 kHz.

Data analysis. Current records were subject to a low-pass Bessel software filter (f_c = 200 Hz) in Clampfit 9 before export for further analysis using IgorPro v3.16 (Wavemetrics Inc., OR, USA). The power spectra of currents were calculated from 2048 data point segments of record, as described previously [32,33]. The power spectrum of the activated current was calculated by subtraction of the mean spectrum of the background current from the mean spectrum of currents in the presence of the agonist cocktail or PKA. The power spectra of the activated currents were fitted with a double Lorentzian function:

$$S(f) = \frac{S(0)_1}{1 + (f/f_{c1})^2} + \frac{S(0)_2}{1 + (f/f_{c2})^2}, \quad (1)$$

where $S(0)_1$ and $S(0)_2$ are constants with units of A^2 s, f represents frequency with units of Hz and f_{c1} and f_{c2} are the corner frequencies for each of the two components. The variance of the current was calculated as the integral of the power spectrum. The unitary current was calculated as:

$$i = \sigma^2/\Delta I_p, \quad (2)$$

where i is the unitary current, σ^2 represents the current variance and ΔI_p, the mean activated pipette current calculated as the difference between the pipette current in the presence and absence of PKA-agonism. Noise analysis of the non-stationary currents during activation was performed as described previously [33]. The current variance was calculated for 2048 data point segments of the record and plotted against the corresponding mean pipette current. The relation was then fitted with the relation:

$$\sigma^2 = iI_p - I_p^2/N, \quad (3)$$

where N is the number of channels in the patch and I_p is the mean pipette current (*i.e.* $I_p = i \times N \times P_o$, where P_o represents the channel open probability). Average data are expressed as mean (±SEM).

Results

Scanning ion conductance images were produced from 36 cells (Fig. 1). Indentations in the cell surface parallel to the transverse axis could be clearly discerned in 31 of these cells (marked with a 'z' in Fig. 1). The trough to trough distance was 1.86 ± 0.07 μm (n = 31), consistent with the transverse indentations representing so-called 'z-grooves' [19,29]. After having obtained the image, giga-seals were achieved in 18 of the 36 cells; 4 of these being from the mouths of t-tubules, 4 from the z-grooves and 3 from the region between the z-grooves. It was not possible to identify the region in which the seal had been made in seven recordings; five of these were because no z-grooves were apparent (*Note:* 100% success rate in achieving giga-seals in cells without apparent z-grooves.) and two were due to the cell moving between imaging and seal formation.

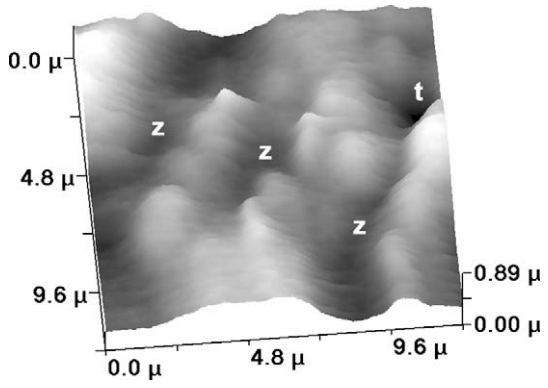

Fig. 1. Representative scanning ion conductance image of a 10 μm square area of the surface of a guinea-pig ventricular myocyte. Letters 'z' indicate grooves in the cell surface and the letter 't' indicates the mouth to a t-tubule.

Superfusion with a cocktail of PKA agonists comprising 5 μM ISO, 10 μM FSK and 50 μM IBMX activated large, noisy currents in 5 of 18 cells (Fig. 2). Currents typically activated rapidly and recovered on washout of the agonist cocktail (marked by '∗' and '#' in Fig. 2A), without clearly defined unitary currents being evident at any stage of current activation. Occasionally, the currents would spontaneously decay in the continued presence of the agonist (*e.g.* '%' in Fig. 2Ai) or re-activate during washout of the agonist (*e.g.* '$' in Fig. 2Aii). The current–voltage relations in the steady state were assessed by recording currents during 3 s voltage pulses from the pipette holding potential of 0 mV (*e.g.* Fig. 2B). The current–voltage relation was linear with a mean reversal potential of −32.1 ± 3.2 mV (n = 5), consistent with the contribution of anion-selective channels to the currents (Fig. 2C). Of the five recordings of currents activated by PKA-agonism, one recording was made from a z-groove (data shown in Fig. 2A and B), one recording was from the region between grooves and three recordings were from regions that it was not possible to identify. No channels were activated in the four recordings from the mouths of t-tubules.

The activated currents were typically large and noisy and no unitary current events could be identified from any of the recordings. Analysis of the power spectrum of the activated currents was performed at each membrane potential (Fig. 3A). The power spectra of the currents could be fitted by a double Lorentzian equation (Eq. (1)) with no obvious voltage-dependence to the corner frequencies (Fig. 3B). For example, the mean corner frequencies for the 5 cells at a membrane potential of −80 mV were f_{c1} = 2.45 ± 0.85 Hz and f_{c2} = 44.10 ± 5.50 Hz and at a membrane potential of +100 mV were f_{c1} = 2.16 ± 0.85 Hz and f_{c2} = 55.94 ± 16.51 Hz. The unitary currents (i) at each membrane potential (V) were calculated from the integral of the power spectra using Eq. (3). Fig. 3C shows the mean unitary current–voltage relation for the 5 cells. The chord conductance for the channels, calculated from the slope of the regression lines fitted to the i–V relations was 13.5 ± 0.7 pS (n = 5). Thus, the data presented hereto in Figs. 2 and 3 suggest that the currents activated by PKA-agonism represent currents carried by a large number of ∼13 pS anion-selective channels gating together. Noise analysis of the non-stationary currents was conducted to obtain an estimate of the numbers of channels underlying these currents (*e.g.* Fig. 3D). The calculated numbers of channels for the five recordings ranged from 58 to 278, with a median of 142 (the mean channel number was 163.2 ± 40.6).

Patch excision from the cell into control excised patch recording solution resulted in complete loss of channel activity, which could not be restored by exposure of the cytosolic surface of the patch to

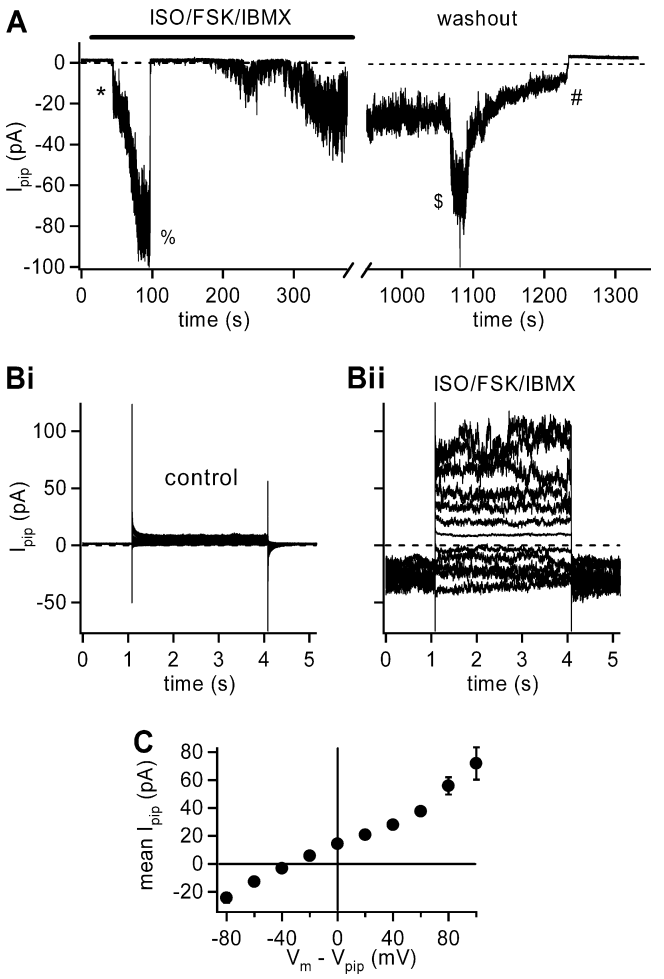

Fig. 2. Currents recorded in cell-attached configuration activated by a cocktail of isoprenaline (ISO, 5 μM), forskolin (FSK, 10 μM) and isobutylmethylxanthine (IBMX, 50 μM). (A) Representative current traces recorded at the resting membrane potential (*i.e.* pipette potential = 0 mV). Dotted lines indicate zero current level. Trace showing activation of current during superfusion with the cocktail of ISO, FSK and IBMX and its recovery on washout of the cocktail. ∗ indicates rapid activation of current. % indicates spontaneous decay of current. $ indicates spontaneous re-activation of currents. # indicates the final deactivation of the current. Note the broken time scale: in this period, depolarizing pulses were applied to obtain current records as shown in Bii below. (B) Currents recorded at pipette potentials from 0 to −180 mV in 20 mV increments before (Bi) and during (Bii) superfusion with the activating cocktail (traces from the same cell as shown in (A)). (C) Current-membrane potential relations of currents activated by the ISO/FSK/IBMX cocktail. Data are the mean (±SEM) from 5 cells.

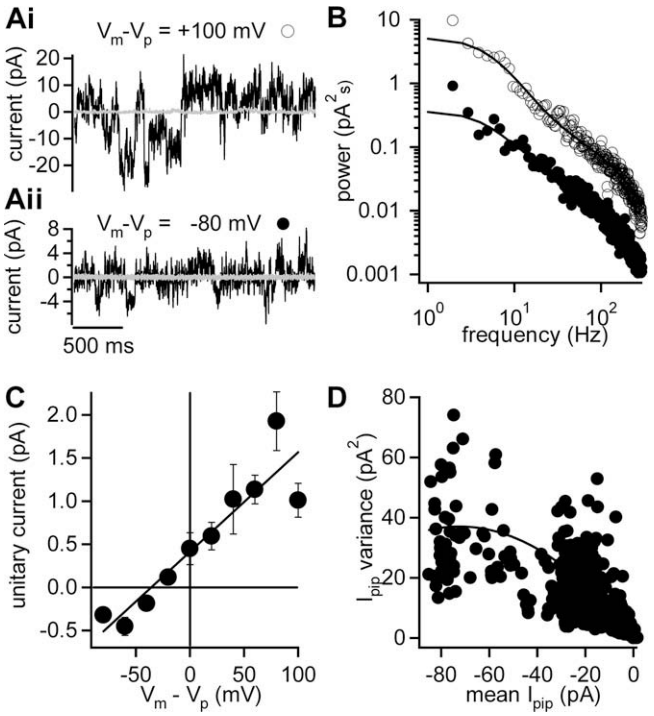

Fig. 3. Noise analysis of ISO/FSK/IBMX-activated currents. Power spectral analysis of ISO/FSK/IBMX-activated currents. (A) Example current traces, with DC component subtracted, recorded before (gray) and during (black) superfusion with ISO, FSK and IBMX at membrane potentials of (i) +100 mV and (ii) −80 mV. Data from the same cell as shown in Fig. 2B. (B) Example power spectra from the data shown in (A). Open circles, data at +100 mV; filled circles, data at −80 mV. Solid lines represent fits to Eq. (1). (C) Unitary current–voltage relations from 5 cells. Data are the means (±SEM) of unitary currents; unitary currents were calculated by power spectral analysis and using Eq. (2). Solid line was fitted by linear least-squares regression. (D) Example non-stationary noise analysis of ISO/FSK/IBMX-activated currents at the resting membrane potential (data shown corresponds to Fig. 2A). Solid line represents a fit to Eq. (3). In this cell, i was −0.49 pA and N was 142.

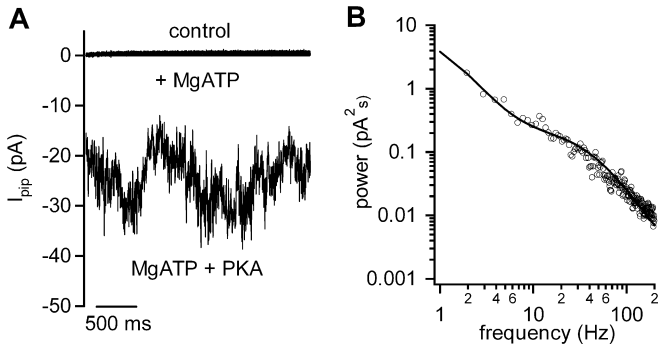

Fig. 4. PKA-activated currents in excised patches. (A) Example current traces recorded in control solution, in the presence of Mg-ATP and in the presence of Mg-ATP with the catalytic subunit of PKA. Membrane potential was −80 mV. (B) Power spectrum of PKA-activated current. Solid line represents a fit to Eq. (1) (f_{c1} = 1.02 Hz; f_{c2} = 38.30 Hz).

Mg-ATP (Fig. 4A). However, addition of the catalytic subunit of PKA in the continued presence of Mg-ATP resulted in the activation of large and noisy currents similar to those seen in cell-attached recordings (Fig. 4A). The power spectrum of the PKA-activated current was remarkably similar to those obtained from recordings in the cell-attached configuration (Fig. 4B).

Discussion

These data demonstrate for the first time that Cl_{PKA} channels in cardiac myocytes occur in clusters consisting of large numbers of channels (>50) in the sarcolemma. The dependence of the currents on PKA-agonism (Figs. 2A and 4), the anion-selectivity (Fig. 2C), the single channel conductance (Fig. 3C) and the properties of the power spectra (Fig. 3B) were all consistent with these representing currents through cardiac CFTR Cl^- channels [6–8,34]. Moreover, the loss of channel activity on patch excision with subsequent recovery on exposure of the cytosolic surface of the patch to the catalytic subunit of PKA argues strongly for the involvement of PKA-dependent channels in the currents (Fig. 4). The single channel conductance of 13.5 pS was remarkably similar to the values of 12–13 pS reported previously for the adrenaline-activated anion unitary currents recorded in the cell-attached mode and the PKA-dependent currents recorded in giant excised patches from this cell type [4,8]. The power spectra were fitted with a double Lorentzian equation with corner frequencies of approximately 2 and 50 Hz, similar to values reported for wild-type human CFTR [34].

Evidence for clusters of channels

Non-stationary noise analysis indicated that the large, noisy currents could be accounted for by the contribution of, on average, 163.2 channels to each activated current. The currents were activated by PKA-agonism in 5 of 18 giga-seals. However, currents were *not* activated in each giga-seal patch, there being 13 giga-seals in which no current whatsoever was activated. Since, if the channels were homogeneously distributed in the membrane, it is very unlikely that 13 recordings could be obtained without any channel activation whatsoever, these data provide very strong evidence that the channels were heterogeneously distributed into clusters in the sarcolemma. These findings are consistent with the proposal that the CFTR Cl^- channel protein interacts with the cytoskeleton, and thereby forms immobilized macromolecular complexes [26–28]. Although, due to the small sample size of the present study, it is not possible to determine the relative distribution of channel clusters between the mouths of t-tubules, z-grooves and the inter-groove region, activated currents were observed in recordings from both the latter regions.

Potential functional significance of channel clusters

The rapid activation of the currents on superfusion with the agonist cocktail in the present study, together with the rapid deactivation on washout, suggests that the channels within the clusters activated together. The PDZ-binding domain of CFTR plays a key role in the interaction of the channel with regulatory proteins, such as PKA [35,36]. Furthermore, there is evidence that the association of CFTR with NHERF/EBP50 itself modulates channel gating [37]. Thus, the clusters of channels may represent large macromolecular complexes incorporating regulatory proteins key to the modulation of channel activity, allowing the activation of relatively large currents through spatially compartmentalized signals. However, both the proportion of giga-seals in which currents were activated (>27%) and the average numbers of channels activated in each recording (typically >50 channels) in the present study were very much greater than those observed or reported by Ehara et al. in their cell-attached recordings of Cl_{PKA} channel currents activated by the physiological agonist, adrenaline, in which typically 3–5 channels were observed in fewer than 5% of recordings [4]. While the reason for the differences in apparent Cl_{PKA} channel density between this and previous studies remains unclear, it is possible that the agonist cocktail used in the present study, comprising a β-adrenoceptor agonist, an adenylyl cyclase activator and a phosphodiesterase inhibitor in combination, led to recruitment of a greater number of Cl_{PKA} channel clusters, and greater number of channels within each cluster, than was possible with adrenoceptor activation using adrenaline alone [4]. In any case, the observation in the present study of large, noisy currents in excised patches activated by exposure of the cytosolic surface of the membrane to the catalytic subunit of PKA (*e.g.* Fig. 4) confirms the existence of clusters of greater than 50 channels in the sarcolemma. Although, in their giant excised patch recordings of cardiac Cl_{PKA} activity, Gadsby and co-workers obtained currents typically involving fewer than 10 Cl_{PKA} channels, these patches were obtained from membrane 'blebs' in which the sarcolemma had become dissociated from the myofilaments; it is therefore possible that the distribution of membrane proteins within the blebs had become disrupted through dissociation from the cytoskeleton, leading to a lower number of channels in each cluster [8,38]. The differences in apparent CFTR channel density between this and previous studies might be explained if; (i) there is a redundancy in CFTR channel expression in guinea-pig ventricular myocytes and/or (ii) not all channel clusters are effectively coupled with β-adrenoceptors. For example, it is possible that the Cl_{PKA} channel clusters co-localized with histamine H_2-receptors would not have been activated when adrenaline was used as the agonist [4,9–11]. Alternatively, co-activation of α_1-adrenoceptors by adrenaline may have limited the effectiveness of this agonist in activating Cl_{PKA} channels [9].

In summary, this study presents novel evidence from cell-attached and excised patch recordings suggesting that CFTR Cl_{PKA} channels in guinea-pig cardiac myocytes occur in spatially discrete clusters involving large numbers of channels (typically >50 channels/cluster). Further investigation of the activation of the CFTR Cl_{PKA} channel clusters in cardiac myocytes by physiological agonists is warranted in the future.

Acknowledgments

Thanks are due to Professors Tsuguhisa Ehara (Saga) and David Gadsby (New York) for discussion of the data, to Professor Yuri Korchev (London) for supplying an update to the Imag software and to Dr. David Sheppard and Professor Neil Marrion (Bristol)

for comments on the manuscript. This work was supported by Grants-in-Aid for Scientific Research (A) and (C) to YO and RZS from MEXT, Japan. AFJ was in receipt of a Visiting Professorship from the Japanese Government and support from CNPq (Brazil).

References

[1] R.D. Harvey, C.D. Clark, J.R. Hume, Chloride current in mammalian cardiac myocytes: novel mechanism for autonomic regulation of action potential duration and resting membrane potential, J. Gen. Physiol. 95 (1990) 1077–1102.
[2] A. Bahinski, A.C. Nairn, P. Greengard, D.C. Gadsby, Chloride conductance regulated by cyclic AMP-dependent protein kinase in cardiac myocytes, Nature 340 (1989) 718–721.
[3] S. Matsuoka, T. Ehara, A. Noma, Chloride-sensitive nature of the adrenaline-induced current in guinea-pig cardiac myocytes, J. Physiol. (Lond.) 425 (1990) 579–598.
[4] T. Ehara, K. Ishihara, Anion channels activated by adrenaline in cardiac myocytes, Nature 347 (1990) 284–286.
[5] D. Duan, Phenomics of cardiac chloride channels: the systematic study of chloride channel function in the heart, J. Physiol. (Lond.) 587 (2009) 2163–2177.
[6] A.F. James, T. Tominaga, Y. Okada, M. Tominaga, Distribution of cAMP-activated chloride current and CFTR mRNA in the guinea pig heart, Circ. Res. 79 (1996) 201–207.
[7] P. Hart, J.D. Warth, P.C. Levesque, et al., Cystic fibrosis gene encodes a cAMP-dependent chloride channel in heart, Proc. Natl. Acad. Sci. USA 93 (1996) 6343–6348.
[8] G. Nagel, T.-C. Hwang, K.L. Nastiuk, A.C. Nairn, D.C. Gadsby, The protein kinase A-regulated cardiac Cl^- channel resembles the cystic fibrosis transmembrane conductance regulator, Nature 360 (1992) 81–84.
[9] L.M. Oleksa, L.C. Hool, R.D. Harvey, α_1-Adrenergic inhibition of the β-adrenergically activated Cl^- current in guinea pig ventricular myocytes, Circ. Res. 78 (1996) 1090–1099.
[10] A.F. James, L.-H. Xie, Y. Fujitani, S. Hayashi, M. Horie, Inhibition of the cardiac protein kinase A-dependent chloride conductance by endothelin-1, Nature 370 (1994) 297–300.
[11] T.-C. Hwang, M. Horie, A.C. Nairn, D.C. Gadsby, Role of GTP-binding proteins in the regulation of mammalian cardiac chloride conductance, J. Gen. Physiol. 99 (1992) 465–489.
[12] M. Tominaga, M. Horie, S. Sasayama, Y. Okada, Glibenclamide, an ATP-sensitive K^+ channel blocker, inhibits cardiac cAMP-activated Cl^- conductance, Circ. Res. 77 (1995) 417–423.
[13] C.H. Orchard, M. Pasek, F. Brette, The role of mammalian cardiac t-tubules in excitation–contraction coupling: experimental and computational approaches, Exp. Physiol. 94 (2009) 509–519.
[14] F. Brette, C. Orchard, T-tubule function in mammalian cardiac myocytes, Circ. Res. 92 (2003) 1182–1192.
[15] A. Maguy, T.E. Hebert, S. Nattel, Involvement of lipid rafts and caveolae in cardiac ion channel function, Cardiovasc. Res. 69 (2006) 798–807.
[16] P.A. Insel, B.P. Head, R.S. Ostrom, et al., Caveolae and lipid rafts: G protein-coupled receptor signaling microdomains in cardiac myocytes, Ann. NY Acad. Sci. 1047 (2005) 166–172.
[17] S. Despa, F. Brette, C.H. Orchard, D.M. Bers, Na/Ca exchange and Na/K-ATPase function are equally concentrated in transverse tubules of rat ventricular myocytes, Biophys. J. 85 (2003) 3388–3396.
[18] M. Kawai, M. Hussain, C.H. Orchard, Excitation–contraction coupling in rat ventricular myocytes after formamide-induced detubulation, Am. J. Physiol. 277 (1999) H603–H609.
[19] Y. Gu, J. Gorelik, H.A. Spohr, et al., High-resolution scanning patch-clamp: new insights into cell function, FASEB J. 16 (2002) 748–750.
[20] S. Calaghan, L. Kozera, E. White, Compartmentalisation of cAMP-dependent signalling by caveolae in the adult cardiac myocyte, J. Mol. Cell. Cardiol. 45 (2008) 88–92.
[21] Y. Xiang, V.O. Rybin, S.F. Steinberg, B. Kobilka, Caveolar localization dictates physiologic signaling of beta 2-adrenoceptors in neonatal cardiac myocytes, J. Biol. Chem. 277 (2002) 34280–34286.
[22] H. Tsujikawa, Y. Song, M. Watanabe, et al., Cholesterol depletion modulates basal L-type Ca^{2+} current and abolishes its beta-adrenergic enhancement in ventricular myocytes, Am. J. Physiol. 294 (2008) H285–H292.
[23] K.L. Dodge-Kafka, L. Langeberg, J.D. Scott, Compartmentation of cyclic nucleotide signaling in the heart: the role of A-kinase anchoring proteins, Circ. Res. 98 (2006) 993–1001.
[24] C. Terrenoire, C.E. Clancy, J.W. Cormier, K.J. Sampson, R.S. Kass, Autonomic control of cardiac action potentials: role of potassium channel kinetics in response to sympathetic stimulation, Circ. Res. 96 (2005) e25–e34.
[25] J.T. Hulme, T.W.C. Lin, R.E. Westenbroek, T. Scheuer, W.A. Catterall, b-Adrenergic regulation requires direct anchoring of PKA to cardiac CaV1.2 channels via a leucine zipper interaction with A kinase-anchoring protein 15, Proc. Natl. Acad. Sci. USA 100 (2003) 13093–13098.
[26] F. Sun, M.J. Hug, C.M. Lewarchik, et al., E3KARP mediates the association of ezrin and protein kinase A with the cystic fibrosis transmembrane conductance regulator in airway cells, J. Biol. Chem. 275 (2000) 29539–29546.
[27] I.R. Bates, B. Hébert, Y. Luo, et al., Membrane lateral diffusion and capture of CFTR within transient confinement zones, Biophys. J. 91 (2006) 1046–1058.
[28] W.B. Guggino, The cystic fibrosis transmembrane regulator forms macromolecular complexes with PDZ domain scaffold proteins, Proc. Am. Thorac. Soc. 1 (2004) 28–32.
[29] J. Gorelik, Y. Gu, H.A. Spohr, et al., Ion channels in small cells and subcellular structures can be studied with a smart patch-clamp system, Biophys. J. 83 (2002) 3296–3303.
[30] G. Isenberg, U. Klockner, Calcium tolerant ventricular myocytes prepared by preincubation in a ''KB medium'', Pflugers Arch. 395 (1982) 6–18.
[31] A.K. Dutta, Y.E. Korchev, A.I. Shevchuk, et al., Spatial distribution of maxi-anion channel on cardiomyocytes detected by smart-patch technique, Biophys. J. 94 (2008) 1646–1655.
[32] S.C. Choisy, J.C. Hancox, L.A. Arberry, et al., Evidence for a novel K^+ channel modulated by α_{1A}-adrenoceptors in cardiac myocytes, Mol. Pharmacol. 66 (2004) 735–748.
[33] R.M. Helliwell, W.A. Large, Facilitatory effect of Ca^{2+} on the noradrenaline-evoked cation current in rabbit portal vein smooth muscle cells, J. Physiol. (Lond.) 512 (1998) 731–741.
[34] H. Fischer, T.E. Machen, CFTR displays voltage dependence and two gating modes during stimulation, J. Gen. Physiol. 104 (1994) 541–566.
[35] F. Sun, M.J. Hug, N.A. Bradbury, R.A. Frizzell, Protein kinase A associates with cystic fibrosis transmembrane conductance regulator via an interaction with ezrin, J. Biol. Chem. 275 (2000) 14360–14366.
[36] L.A. Borthwick, J. McGaw, G. Conner, et al., The formation of the cAMP/protein kinase A-dependent annexin 2 S100A10 complex with cystic fibrosis conductance regulator protein (CFTR) regulates CFTR channel function, Mol. Biol. Cell 18 (2007) 3388–3397.
[37] V. Raghuram, D.-O.D. Mak, J.K. Foskett, Regulation of cystic fibrosis transmembrane conductance regulator single-channel gating by bivalent PDZ-domain-mediated interaction, Proc. Natl. Acad. Sci. USA 98 (2001) 1300–1305.
[38] D.W. Hilgemann, Giant excised cardiac sarcolemmal membrane patches: sodium and sodium–calcium exchange currents, Pflugers Arch. 415 (1989) 247–249.